

Time Dependence of CTE from Cosmic Ray Tails

Adam Riess, John Biretta, Stefano Casertano
December 23, 1999

ABSTRACT

We have developed a method to measure the counts in cosmic ray tails (CRTs) which result from imperfect charge transfer efficiency (CTE). Like previous measures of CTE, the counts in the CRTs are a strong function of the number of serial and parallel transfers, background, source counts, and lifetime of the instrument. Analysis of the CRTs reveals that some charge is trapped and released on short timescales (\ll seconds) although the charge in CRTs does not account for all observed CTE losses. The time dependence of Y-CTE and X-CTE are shown for WFPC2 and STIS using the STScI archive of dark calibration frames. All show a steady growth with time since installation of the respective instrument. There is also evidence for a mild increase in the growth rate (i.e. acceleration) of the WFPC2 Y-CTE. The results indicate that this method may provide a precise way to monitor CTE with greater time sampling than is currently feasible and without the cost of additional pointed observations.

1. Introduction

As in Quantum Mechanics, the process of measuring charge on a CCD impacts the value of the measurement. Charge transfer efficiency (CTE) is the term commonly used to describe all losses to a charge packet caused by traversing an array of pixels. Classic CTE is quantified by the fraction of charge which successfully moves (clocks) between pixels during a single transfer (and therefore CTI or charge transfer *inefficiency* is $1 - \text{CTE}$). Knowledge of the current value of CTE would allow one to restore the values of charge packets to their pre-measured values. However, physical charge transfer is more complex. Investigations have revealed that charge which fails to transfer between pixels becomes “trapped” for time periods surpassing subsequent clockings (Biretta & Mutchler 1998).

Out of necessity, investigators have derived empirical correction formulae which calibrate the losses to a charge packet as a function of the number of serial and parallel

clockings, background (which can fill in traps) and the size of the charge packet (which may determine how many traps are accessible; e.g., Whitmore, Heyer, & Casertano 1999, hereafter WHC99).

WFPC2

Extensive CTE analysis has been done on the WFPC2 on HST and for good reasons. The Earth's atmosphere which blurs astronomical images also protects ground-based CCDs from radiation damage. Cosmic rays in the space environment damage the CCD and the overall CTI grows. Past, present, and future users of WFPC2 demand a high degree of precision from their photometric measurements. Therefore the WFPC2 Instrument Team has devoted significant effort and valuable telescope time to insuring that the detrimental effects of CTE can be well-calibrated.

The increase in CTI has been dramatic. Shortly after launch in 1994, Holtzman et al. (1995) derived a simple linear correction (i.e., a ramp) for CTE. A star which traversed the full 800 pixels in the *Y*-coordinate suffered a 4% loss. Continued monitoring by the WFPC2 instrument team revealed growing losses, especially for the faintest sources; by February 1999 stars with 20-50 counts and little background ($\ll 1$ count) were observed to be ~40% fainter at $y=800$ than at $y=1$ (although for typical science exposures which have higher backgrounds the losses are much lower; WHC99). In addition, corrections for CTE as a function of *X*-coordinate, source counts, and background were derived. However, the significant temporal dependence of these corrections makes it critical to continue to monitor CTE so that precise photometric measurements can be made from WFPC2 observations.

Unfortunately, the stellar observations required to monitor CTE losses require valuable pointed telescope time and cannot be performed with enough frequency to be concurrent with all science observations. However, there may be other less costly ways to effectively monitor CTE.

Cosmic rays in dark frames incur CTE losses and a signature of this effect is the "tails" or trails of charge which lag behind the cosmic ray at high *Y* coordinates. Visual inspection of these tails in dark frames (see Figure 1) indicates that the counts in these tails depends on the *Y* position of the cosmic ray. By developing an algorithm to measure the counts in the tails we may be able to develop a better understanding of CTE and add an effective tool to monitoring its time dependence. In the following sections we develop a general technique to measure cosmic ray tails and we apply it to the time dependence of CTE for the WFPC2 and STIS instruments on the HST.

the tails indicates that charge is also trapped and released on shorter time scales (where “short” means of order the clocking time for a CCD row).¹

Unlike the OI and the CD, CTE adds an *asymmetric* component to the cosmic ray image. We can use this asymmetry to separate CTE from the statistically symmetric “noise” of OI and CD.

Our detailed procedure is to flag all pixels above a threshold as “cosmic rays” or high pixels (even though numerous such pixels came from a single cosmic ray event). For each high pixel, we subtract the pixels below from their symmetric counterparts above (i.e. the pixel below is subtracted from the pixel above, the pixel two pixels below is subtracted from the pixel two pixels above, and so on...). This subtraction process *statistically* removes all sources of symmetric “noise”. That is, the expectation is that if we average this process over enough cosmic rays (thereby sampling all angles of incidence and directions of charge diffusion) the difference between pixels above and below any high pixel should be zero. However, the charges trapped and released add a tail of “delayed” charge into pixels at higher Y than the cosmic ray. So from the statistics of many cosmic rays, this subtraction process should measure the average tail on a typical cosmic ray due to CTE. A schematic illustration of this method is shown in Figure 2.

Shown in Figure 3 are these charge differences or excesses around cosmic ray pixels from a single dark frame as a function of the distance from the pixels. The top panel shows these differences for cosmic rays in the lowest 100 rows (Y=1 to 100) and the bottom panel for the top 100 rows (Y=700 to 800). The points are the data while the curve is the median of the data. For the purpose of quantifying the CTE tail we have fit an exponential to this curve and taken the total counts in the tail to be the area under the fitted exponential. As shown in the top panel of Figure 3 (and seen repeatedly in many dark frames), no significant tail is apparent at low Y, validating our assumptions of symmetry for OI and CD. At high Y an exponentially declining tail is readily apparent. In order to make use of all the cosmic rays in each dark frame we have divided each image into eight regions (Y=1 to 100, Y=101 to 200, etc.) and separately fit an exponential to the cosmic ray tail for that region. We then fit a line to the counts in the tail as a function of the mid-point of the bins (Figure 4). The monotonic increase of the counts in the tails with Y (starting from near zero at low Y) again demonstrates that the tails are caused by CTE. We have chosen as our final metric, the expected counts in the cosmic ray tail (CRT) at pixel Y=800.

1. Actually a simple CTE can cause cosmic ray tails without any trapping. In fact, simple CTE lower than 0.9991 for WFPC2 will add a “nose” of charge opposite the tail as the highest pixel at high Y is reduced below half its original intensity and the next pixel becomes the new peak. However, CTE without any short time scale trapping results in tails which decay much faster than the observed tails for any value of CTE as explained in section 3. For that reason alone, it is clear that the cosmic ray tails arise from charge trapping.

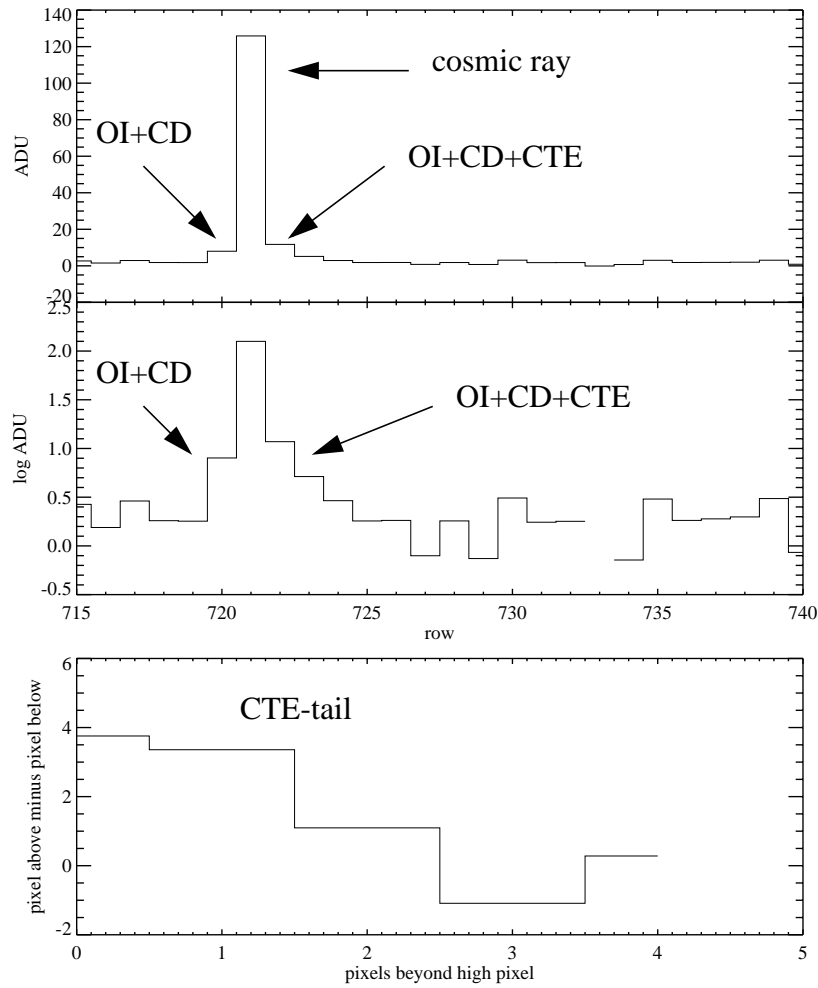


Figure 2: Schematic of method to measure cosmic ray tails. The top two panels show the intensity profile of a typical cosmic ray along a CCD column (i.e., in the Y-direction) plotted linearly and logarithmically. Oblique incidence (OI) of cosmic rays and charge diffusion (CD) spreads charge symmetrically around the peak of a cosmic ray, statistically. CTE creates an asymmetric tail of charge. Subtracting the counts in the pixel after the cosmic ray from those in the pixel before the cosmic ray statistically recovers the CTE-tail (bottom panel).

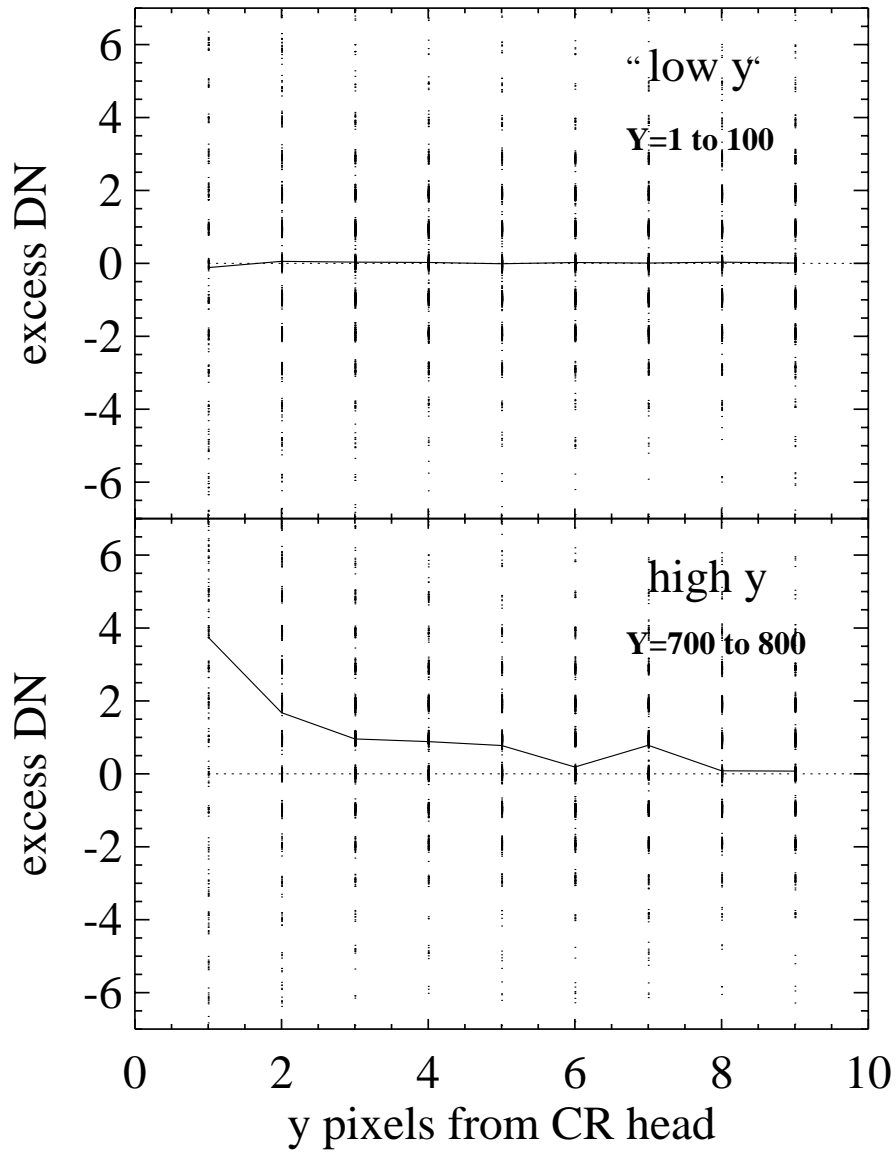


Figure 3: Cosmic ray tails in a single WFPC2 dark frame. Each individual point represents one cosmic ray and shows the differences between pixels which are equal distances from a cosmic ray pixel. The line is the median of the data. At low Y there are few charge transfers and hence minimal trailing of charge. At high Y the statistical cosmic ray tails are evident from one dark frame.

In practice we found that dark frames with exposure times between 200 and 2400 seconds have a sufficient flux of cosmic rays to yield a robust measure of the CRT.

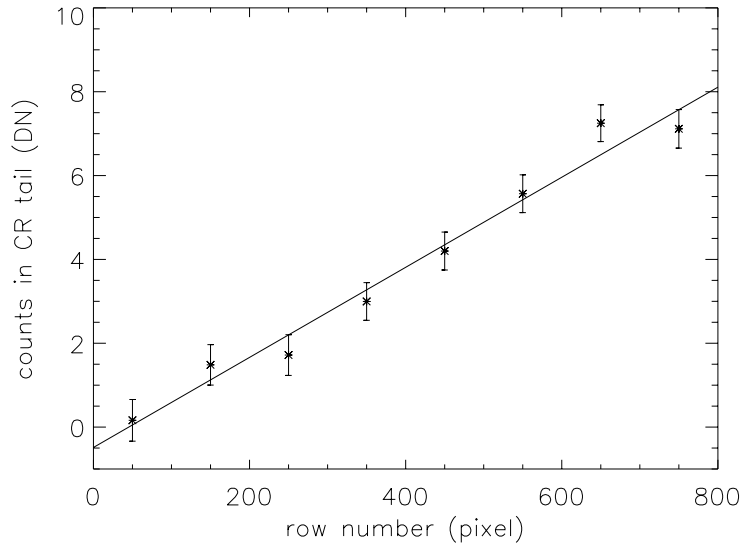


Figure 4: Counts in CTE-tails versus row number. The linear dependence on row number is a clear indication of CTE. The intercept of the fitted line at $Y=800$ is used as a CTE metric.

3. CTE and Cosmic Ray Tail

What can we learn about CTE from the CRT measurements? Lots!

Basic Properties of Cosmic Ray Tails

The length of the cosmic ray tail is a measure of the time scale for charge release from the CCD traps. For WFPC2 we find these tails to have a “length” (i.e., an e-fold decay length) of 2.0 ± 0.4 pixels, indicating that some charge is held and released again on the time scale of 2 WFPC2 parallel clockings, or about 34 milliseconds. As we will also show, the WFPC2 CCDs also have a weaker X-CTE effect, for which the timescale is of order tens of microseconds. From STIS dark frames we have found the length/time-scale to be much greater, approximately 6-7 pixels (about 0.2 seconds).

How much charge is contained in these tails? Like CTE measures from stars (WHC99) the loss of charge from the cosmic ray to the tail is neither a fixed number of counts nor a fixed fraction of the cosmic ray strength, but rather a quantity in between. At gain=7, the median counts in a WFPC2 dark frame for cosmic ray pixels well above the background (threshold=50 DN) is 160 to 180 DN. The current (i.e., November 1999) tails contain a total of 6 to 7 counts, hence comprising about 4% of the counts. We can examine the fractional size of the tails in different cosmic ray intensity bins. We find that at a cosmic ray intensity of 20 DN the tail contains about 5% of the counts, whereas at 1000 DN the tail is about 1% of the counts.

Like the stellar CTE measurements, the cosmic ray tail metric for CTE is a strong function of the background counts. We analyzed the CRTs of coeval dark frames from 200 to 2400 seconds whose dark current background varies from 0.1 to 2.0 DN. In addition we measured CRTs from coeval science exposures with median backgrounds up to 15 DN. As seen in Figure 5 the counts in the tails decrease monotonically with increased background, but remain detectable at median background DN=15. Presumably the background counts fill traps, reducing the losses to cosmic ray counts. However, there are probably deeper traps which cannot be filled by the background but are accessed by the larger charge packets of cosmic ray.

Current estimates for the CTE losses for stars with similar source counts and backgrounds as for the cosmic rays in the WFPC2 dark frames are about 10%. It is therefore unlikely that the charge in the tails can account for the total of the losses found from stellar measurements. Further, much of the charge in the tails would *not* be lost to stellar photometry with aperture radii of several pixels. For WFPC2, apertures of radius greater than the 2 pixel e-fold decay length will include most of the charge in the tails. However, the differences in the values of total CTE loss in stellar measurements reported in the literature may result from differences in the size of small apertures used to measure the photometry, or whether an empirical PSF model is used (see WHC99; Stetson 1998.)

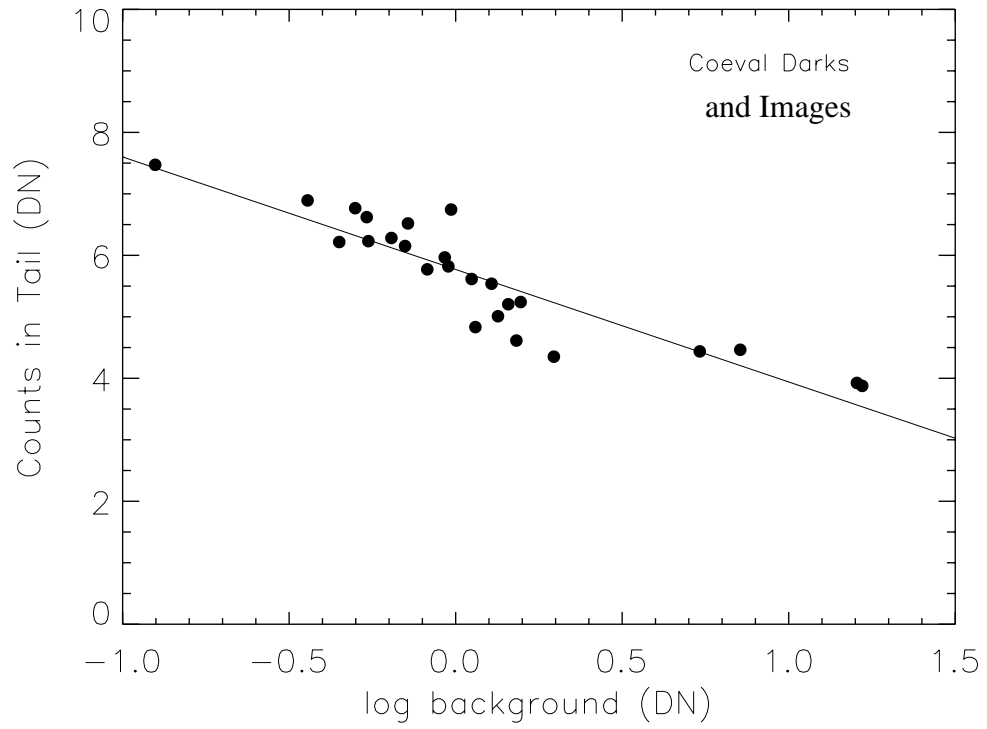


Figure 5: Dependence of counts in CTE-tails on background level in image. Data are all from 09/98 to 11/98.

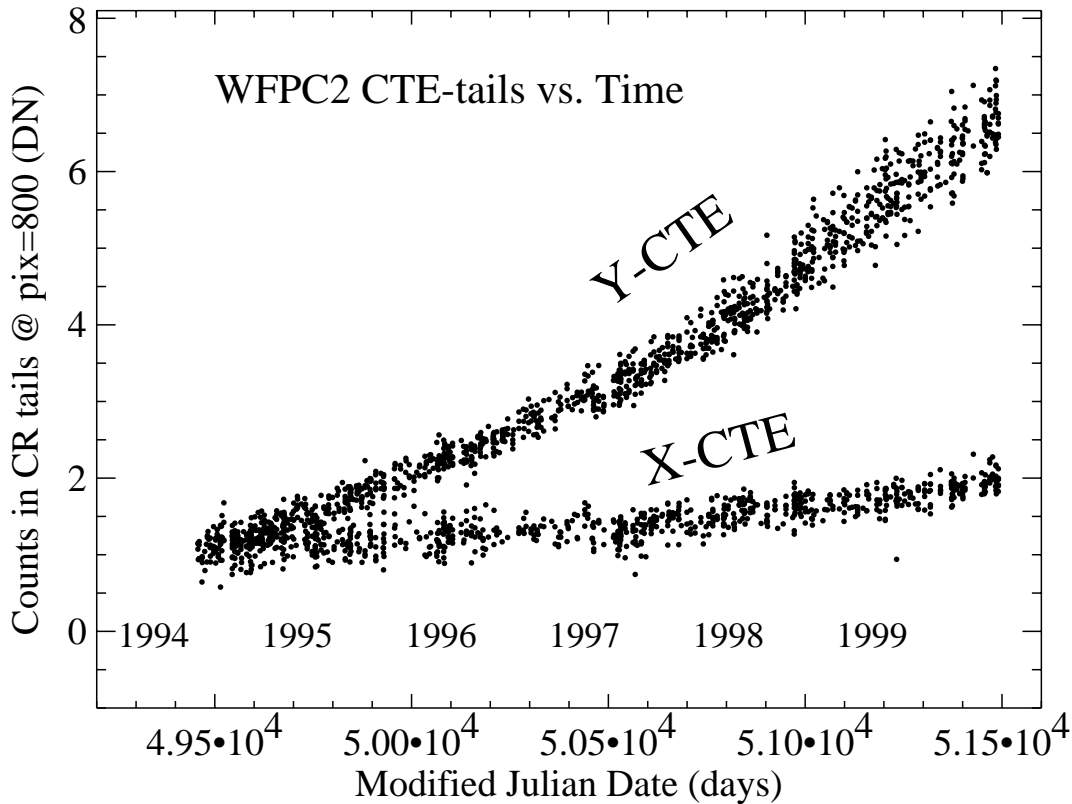


Figure 6: The growth of the counts in CTE-tails of cosmic rays as a function of time. Each point is derived from a single WFPC2 dark frame. The upper points are for Y-CTE and the lower ones are for X-CTE.

Long-term Time Dependence

We have applied the methods described above to measure the counts in the cosmic ray tails as a function of time for both WFPC2 and STIS. A clear advantage of exploring the time dependence of CTE using this method is that there are thousands of dark frames in the STScI archive which have been taken from shortly after installation of the instruments to the present time. The dark frames from WFPC2 and STIS can provide a detailed historical record of the growth of CTE.

Figure 6 displays the temporal dependence of both parallel-read (Y) and serial-read (X) induced-tails for WFPC2. The CRT metric sharply delineates the detailed growth of CTI. Like stellar CTE measurements (WHC99), the cosmic ray CTE tails were detectable after installation and have been growing with time. They may even show some mild accel-

eration in the sense that the current counts in the CR tails are somewhat higher than expected by the extrapolation of the linear growth up to 1998. It is important to note that all of these dark frames have identical exposure times of 1800 seconds and very similar median background counts. The same growth trend is seen in Figure 6 for X-CTE tails except the size of the X-tails are much smaller and have presently converged at 1/3 the size of the Y-tails, in good agreement with the relative strengths of X to Y stellar CTE measurements (WHC99). In Figure 7 we display the time dependence of the STIS CTE-tails measured from cosmic rays in dark frames. The X-CTE for STIS is a full magnitude lower than Y-CTE, consistent with the photometric CTE measurements of Gilliland, Goudfrooij & Kimble (1999). The Y-CTE for STIS displays a strong linear growth with time.

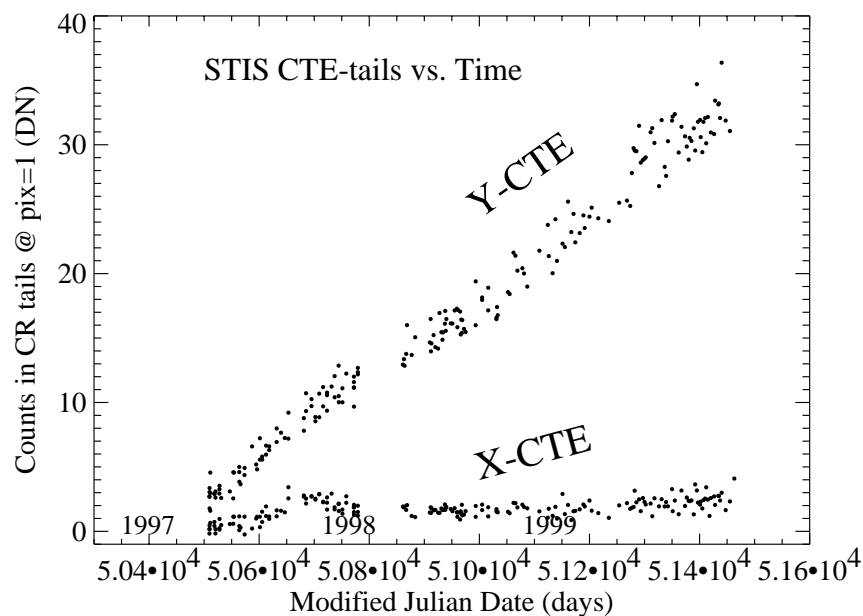


Figure 7: Same as Figure 6 but for STIS

Further investigations will look for sub-structure in the temporal growth of the CTE-tails. For example, is there a reduction in CTE after decontaminations? What is the dependence of CTE on temperature? Does CTE vary from chip to chip for WFPC2? Can sources fill traps and reduce CTE for other sources in the same column?

4. Discussion

The results of the previous section indicate that the counts in cosmic ray tails track photometric CTE because they result from trapping, increase with Y and X pixel number, are reduced in the presence of background and have been growing with time. However, it appears that cosmic ray tails may result from a shorter time scale trapping than does stellar CTE measurements since the counts in the tails represent only a fraction of the stellar CTE effect.

The CTE-tail measurements described here are not a replacement for stellar CTE measurements but rather could be used as a powerful *predictor* of total CTE. The data required for stellar CTE measurements of the kind performed by WHC99 require valuable HST time. The advantage of using CR tails to monitor CTE is that the dark frames for these observations are already gathered for the purpose of monitoring hot pixels and dark current. Using such data to monitor CTE could provide greater time sampling and a higher precision of calibration of CTE than is currently feasible with less cost of pointed telescope time.

A more far-reaching goal than the empirical monitoring of CTE is the development of a deeper understanding of CTE. The work presented here and elsewhere (Biretta & Mutchler 1998) already indicates that the current CTE problem involves at least two different time-scales of trapping. The residual planet images reported by Biretta & Mutchler (1998) are generated by deep charge packets (~2000 DN) and persist over many minutes. The cosmic ray tails reported here are generated by much smaller charge packets (~170 DN) and decay over tens of milliseconds (or tens of microseconds for X-CTE). One reasonable hypothesis is that there is a *continuum* of traps at different depths within each a pixel. Perhaps the deepest traps are only accessed by larger charge packet. It is also evident that different traps have different timescales to release charge, and this could conceivably be a related to the depth of the trap. Such a hypothesis could explain why background counts seem to alleviate CTE most effectively for sources with similar counts as the background.

In the future it may also be possible to use diagnostics of CTE like stellar measurements, residual images, and cosmic ray tails to build a useful model of the read-out process (i.e. the mapping between the image before and after CTE effects). Such a model would be very useful for understanding how to restore more complex scenes which include extended objects or stellar objects in regions of variable background.

Acknowledgements: We thank Ron Gilliland and John MacKenty for useful discussions.

References

Biretta, J. and Mutchler, M. 1998, Charge Trapping and CTE Residual Images in the WFPC2 CCDs, WFPC2-ISR-97-05

Gilliland, R. L., Goudfrooij, P., & Kimble, R. A., 1999, PASP, 111, 1009

Holtzman, J. A., Burrows, C., Casertano, S., Hester, J. J., Trauger, J. T., Watson, A. M., & Worthey, G., 1995, PASP, 107. 1065

Stetson, P. B., 1998, PASP, 110, 1448,

Whitmore, B., Heyer, I., & Casertano, S., 1999, PASP, in press